Charge-Transfer Character in the Intramolecular Hydrogen Bond: Vacuum Ultraviolet Spectra of Acetylacetone and Its Fluoro Derivatives

Hiroshi NAKANISHI, Hiroshi MORITA, and Saburo NAGAKURA

The Institute for Solid State Physics, The University of Tokyo, Roppongi, Minato-ku, Tokyo 106

(Received January 28, 1978)

Near and vacuum UV absorption spectra of trifluoroacetylacetone (TFAC) and hexafluoroacetylacetone (HFAC) were measured at room temperature in the vapor phase and in perfluorohexane in the 30000—80000 cm^{-1} region, together with a vacuum UV absorption spectrum of acetylacetone in the 60000—80000 cm^{-1} region. By the aid of the modified CNDO-CI calculation, each of the observed valence-shell transition bands was assigned to the π–π^*, π–σ^*, or σ–σ^* transition. The third σ–σ^* bands observed at 65200 cm^{-1} for acetylacetone, at 78000 cm^{-1} for TFAC, and at 70400 cm^{-1} for HFAC were concluded to be rich in the CT character pertinent to hydrogen bond. In particular, the third σ–σ^* band of HFAC was found to be the CT band pertinent to hydrogen bonding in the sense that the contribution of the CT configuration to the excited state amounts to 67.4%.

Importance of the charge-transfer (CT) mechanism in hydrogen bond has been recognized by many authors from theoretical[1–7] and experimental[8–10] points of view. The CT mechanism can strongly be supported by the observation of the CT band pertinent to hydrogen bond.[11] The CT character of intramolecular hydrogen bond in the ground and excited electronic states was investigated for the hydrogen maleate anion;[12,13] the theoretical and experimental results indicated that the first π-π^* band which is rich in the CT character pertinent to the hydrogen bond is covered by the strong second π-π^* band at 210 nm.[13]

The enol forms of acetylacetone, trifluoroacetylacetone (TFAC), and hexafluoroacetylacetone (HFAC) have a strong intramolecular hydrogen bond with the O···O distance of 2.38—2.55 Å as revealed from X-ray diffraction[14] and gas-phase electron diffraction studies.[15,16] In a previous paper,[17] we reported the electronic structures and spectra of the keto and enol forms of acetylacetone in the 30000—61000 cm^{-1} region, and discussed the CT character of the intramolecular hydrogen bond of the enol form. Concerning the electronic structures and spectra of the fluoroacetylacetones, only a few studies have been made.[18–20]

Our previous study[17] of the electronic structure and spectrum of acetylacetone led us to the expectation that a band rich in the CT character might appear in a higher energy region than 61000 cm^{-1}. In the present paper, we extend the spectral region to 80000 cm^{-1} in the vacuum ultraviolet (VUV) region and measure the absorption spectra of acetylacetone in the vapor phase and of TFAC and HFAC in the vapor phase and in perfluorohexane. From analysis of the experimental results by the modified CNDO-CI method[21] and the configuration analysis method,[22] the nature of the valence-shell transition and Rydberg excitation bands is discussed, special attention being paid to the identification of the CT band pertinent to the intramolecular hydrogen bond.

Experimental

Materials. TFAC (Dotait G.R. Grade) and HFAC (Dotait G. R. Grade) were purified by repeating vacuum distillation three times immediately before use. Acetylacetone and perfluorohexane were purified in the same way as reported previously.[17]

Measurement. Near UV (30000—50000 cm^{-1}) absorption spectra were measured with a Cary recording spectrophotometer Model 14. VUV (50000—80000 cm^{-1}) absorption spectra were measured with a Johnson-Onaka type VUV spectrophotometer,[23] the sample chamber and detector system of which were modified as shown in Fig. 1. A hot cathode deuterium discharge lamp and Tanaka type xenon and krypton continuum lamps driven with microwave excitation (2450 MHz) were used as VUV light sources. Cells with MgF_2 or LiF windows of 5—10 cm light path lengths and a 0.01 cm quartz cell were used for the measurement in the vapor phase and in the solution, respectively. The vapor pressure of the sample was regulated with a cryogenic bath at various temperatures.

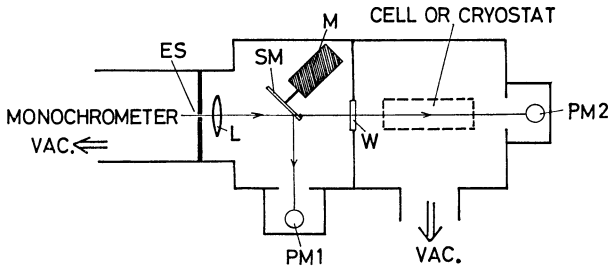

Fig. 1. Schematic diagram of the sample chamber and detector system of the VUV spectrophotometer. ES; Exit slit, L; MgF_2 lens (f=60 mm), SM; rotating sector mirror, M; oilless motor, W; MgF_2 window, PM 1 and 2; photomultipliers (HTV R106) coated with sodium salicylate.

Theoretical

The modified CNDO-CI method[21] was applied to the enol forms of acetylacetone, TFAC, and HFAC to investigate the valence-shell transitions. The semiempirical parameters of H, C, and O atoms were the same as reported previously.[17,21] The parameters of F atom were adopted as follows; the one-center Coulomb repulsion integral, γ_F=19.36 eV, the bonding parameter, β_F^0=−40.0 eV, and the $(I+A)/2$ values, 32.772 eV for the 2s AO, and 11.580 eV for the 2p AO. Preliminary calculations for such fluorinated molecules as carbon

tetrafluoride, carbonyl fluoride, trifluoroacetoaldehyde, and trifluoroacetic acid with the use of these parameters showed that the calculated transition energies and oscillator strengths agree well with the observed values. In the configuration interaction (CI) treatment of TFAC and HFAC, 40 singly excited π-π^* and σ-σ^* configurations and 40 singly excited π-σ^* and σ-π^* configurations were taken into account.

The actual calculations were made for two different geometrical structures, symmetrical and asymmetrical ones. Symmetrical molecular structures of TFAC and HFAC were taken from the results of gas-phase electron diffraction studies,[15] the linear symmetrical intramolecular hydrogen bond, O···H···O being assumed, and asymmetrical molecular structures were taken from the results by nonempirical calculations,[24,25] a non-linear asymmetrical intramolecular hydrogen bond being taken from the X-ray diffraction study.[26]

The configuration analysis was applied to the third σ-σ^* excited state (calculated at 9.02 eV)[17] of the enol form of acetylacetone. The procedure for the analysis was described in detail in the previous paper.[17]

Results and Discussion

The VUV Absorption Spectrum of Acetylacetone. Figure 2 shows the VUV spectrum in the 50000—80000 cm^{-1} region measured with acetylacetone in the vapor phase at room temperature. Since acetylacetone predominantly exists as the enol form in the vapor phase (96.2% at 20 °C),[17] the spectrum in Fig. 2 is ascribed to the enol form. We can see from Fig. 2 that strong bands appear at 65200 cm^{-1} (8.08 eV) and $\approx$79000 cm^{-1} ($\approx$9.8 eV) and shoulders at $\approx$60000 cm^{-1} ($\approx$7.4 eV) and $\approx$71000 cm^{-1} ($\approx$8.8 eV). Table 1 shows theoretical values of the transition energies and oscillator strengths of the valence-shell transition bands, together with the observed values (for the theoretical and observed results below 8 eV, see Table 1 in Ref. 17). From the comparison between the observed and calculated results, the strong 8.08 eV band (oscillator strength, $f\approx0.5$) can safely be assigned to the third σ-σ^* transition (calculated at 9.02 eV) because of its large oscillator strength among the bands calculated in 7.5—10.0 eV region. The other three observed bands at $\approx$7.4 eV, $\approx$8.8 eV, and $\approx$9.8 eV can be assigned to the third π-π^* transition (calculated at 8.46 eV), the fourth σ-σ^* transition (calculated at 9.94 eV), and the fourth π-π^* transition (calculated at 10.15 eV), respectively.

Table 1. Transition energies ($^1\Delta E$(eV)) and oscillator strengths (f) observed and calculated for some higher excited states of the enol form of acetylacetone[a]

Assignment	Obsd[b] $^1\Delta E$	Obsd[b] f	Calcd $^1\Delta E$	Calcd f[d]	Main config.[c]
σ(n)-σ^*			8.38	0.002(x)	20—23
π-π^*	$\approx$7.4	$\approx$0.1	8.46	0.120(y)	17—21
σ-π^*			8.58	0.004(z)	(16,13)—21
π-σ^*			8.60	0.009(z)	19—26
σ(n)-σ^*			8.93	0.022(y)	20—(27, 24)
π-σ^*			9.00	0	19—(27, 24)
σ(n)-σ^*	8.08	$\approx$0.5	9.02	0.685(x)	{20—26 14—21
σ-π^*			9.06	0	15—21
π-σ^*			9.78	0.019(z)	19—(28, 23, 25)
σ(n)-σ^*	$\approx$8.8		9.94	0.045(x)	20—(25, 23)
σ(n)-σ^*			10.04	0.006(y)	20—(27, 24)
π-π^*	$\approx$9.8		10.15	0.050(x)	{14—21 20—26
σ-π^*			10.57	0	16—22
σ-π^*			10.69	0.001(z)	(18, 15)—22

a) For lower excited states ($\leq$8 eV), see Table 1 in Ref. 17. b) Observed value in the vapor phase. c) Main electron configurations of the respective excited states are shown. (i, j)-k denotes the singly excited configurations, i-k and j-k, and i-(k, l), the singly excited configurations, i-k and i-l. The shapes of MO's are shown in Fig. 5 in Ref. 17. d) The direction of the transition moment is shown in the parentheses, the x-axis being taken to be parallel to the O···H···O bond within the molecular (x-y) plane.

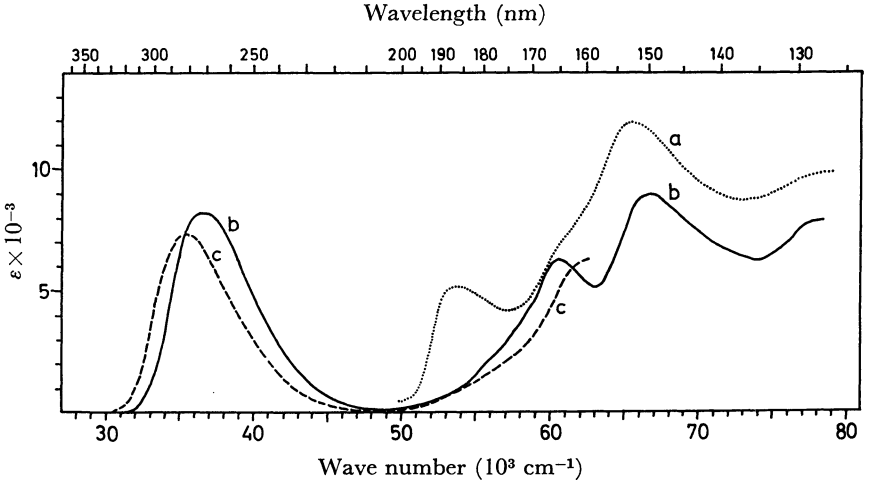

Fig. 2. Near and vacuum UV absorption spectra measured with (a) acetylacetone in the vapor phase, (b) TFAC in the vapor phase, and (c) TFAC in perfluorohexane at room temperature.

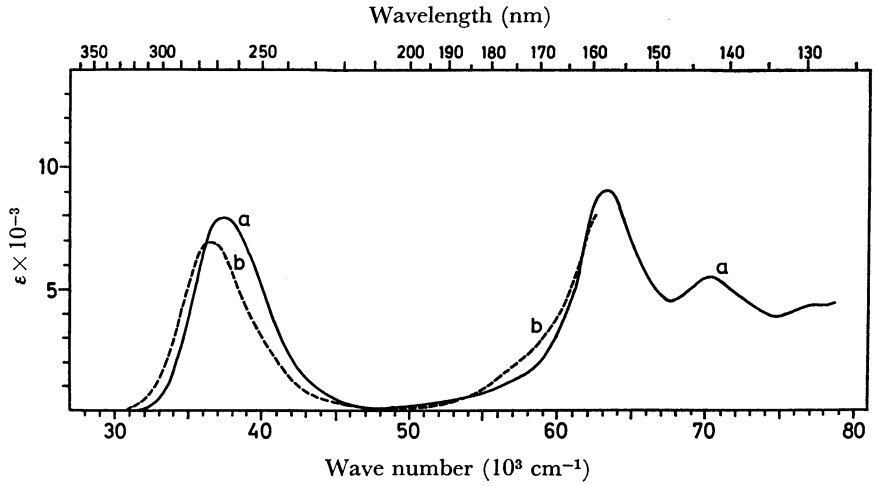

Fig. 3. Near and vacuum UV absorption spectra of HFAC measured (a) in the vapor phase and (b) in perfluorohexane at room temperature.

Electronic Absorption Spectra of TFAC and HFAC. Near and vacuum UV absorption spectra in the 30000—80000 cm^{-1} region measured with TFAC and HFAC at room temperature are shown in Figs. 2 and 3, respectively. As pointed out by the NMR studies,[27,28] substitution of the methyl group(s) in acetylacetone by the more electronegative trifluoromethyl group(s) preponderates the enol tautomer in the keto-enol equilibrium; TFAC and HFAC exist almost completely (95—100%) as the enol form in the vapor phase and in nonpolar solvents at room temperature. Therefore, the observed spectra shown in Figs. 2 and 3 are ascribed to the enol form.

The TFAC vapor spectrum in Fig. 2 has absorption peaks at 36670 cm^{-1} (4.55 eV), 60600 cm^{-1} (7.51 eV), 66700 cm^{-1} (8.27 eV), and 78000 cm^{-1} (9.7 eV), and shoulders at ≈56000 cm^{-1} (≈6.9 eV) and ≈71000 cm^{-1} (≈8.8 eV). The HFAC vapor spectrum in Fig. 3 has absorption peaks at 37450 cm^{-1} (4.64 eV), ≈57000 cm^{-1} (≈7.1 eV) (as a weak shoulder), 63700 cm^{-1} (7.90 eV), 70400 cm^{-1} (8.73 eV), and ≈77000 cm^{-1} (≈9.5 eV).

Comparison between the spectra in the vapor phase and in the solution in Fig. 2 shows that the 60600 cm^{-1} band of TFAC in the vapor phase disappears in the solution. This means that the band is assigned to the Rydberg excitation band.[29] The Rydberg excitation energy satisfies the following formula;[29]

$$h\nu = I_p - 109737/(n-\delta)^2, \quad (1)$$

where $h\nu$ is the excitation energy (cm^{-1}), I_p is the ionization potential (cm^{-1}), n is the principal quantum number, and δ is the quantum defect. By the use of the first I_p value (9.93 eV) determined by photoelectron spectroscopy,[30] the δ value of the 60600 cm^{-1} band was determined to be 0.63, corresponding to $n=3$. This strongly suggests that the band is due to the transition to the 3p Rydberg orbital from the highest occupied π orbital. The band intensity is of the same order of magnitude as the π-3p Rydberg band of acetylacetone[17] observed at 53300 cm^{-1}. The corresponding Rydberg transition band is expected to appear at ≈67000 cm^{-1} for HFAC from the first ionization potential of 10.72 eV.[30] But it is covered by strong valence-shell transition bands and cannot be observed.

Theoretical transition energies and oscillator strengths of the valence-shell transitions of the enol forms of TFAC and HFAC were calculated on the basis of two kinds of (*i.e.*, symmetrical and asymmetrical) molecular structures. The results for lower excited states of both the TFAC and HFAC molecules are rather insensitive to

Table 2. Transition energies ($^1\Delta E$(eV)) and oscillator strengths (f) observed and calculated for the enol form of trifluoroacetylacetone

Assignment	Obsd[a]		Calcd[b]		Main config.[c]
	$^1\Delta E$	f	$^1\Delta E$	f[d]	
σ(n)–π*			2.90	0.000$_6$(z)	29—30
π–π*	4.55	0.18	4.75	0.162 (x$_y$)[e]	28—30
σ(n)–π*			5.17	0.000(z)	29—31
σ–π*			7.35	0.000$_5$(z)	26—30
π–σ*	≈6.9	≈0.03	7.58	0.014(z)	28—32
π–π*	8.27	≈0.25	7.35	0.225(y$_x$)[f]	28—31
σ(n)–σ*			7.99	0.102(x$_y$)[e]	29—32
σ–π*			8.14	0.001(z)	{28—30, 26—31}
σ–π*			8.57	0.016(z)	27—30
π–σ*			8.67	0.004(z)	28—34
π–σ*			8.78	0.017(z)	28—33
σ(n)–σ*	≈8.8		8.97	0.259(x$_y$)[e]	{29—34, 29—33}
σ–π*			9.21	0.009(z)	{24—30, 23—30}
σ(n)–σ*	9.7		9.34	0.372(x)	{29—33, 29—34}
π–σ*			9.57	0.014(z)	28—36
π–π*			9.75	0.310(y)	25—30

a) Observed value in the vapor phase. b) Calculated value for the symmetrical molecular structure of the enol form. c) Main electron configurations of the respective excited states are shown. d) The direction of the transition moment is shown in the parentheses, the x-axis being taken to be parallel to the O···H···O bond within the molecular (x-y) plane as is shown in Fig. 8(a). e) y-Component of the transition moment contributes appreciably to x-component. f) x-Component of the transition moment contributes appreciably to y-component.

the molecular structures, and from semiquantitative view-points, the same conclusions are derived concerning the assignments and characterizations of the observed bands.

Table 2 shows the theoretical results calculated for the symmetrical molecular structure of the enol form of TFAC compared with the observed values. The 4.55 eV band can safely be assigned to the first π-π^* transition (calculated at 4.75 eV) and corresponds to the 4.72 eV band of acetylacetone. The strong 61700 cm^{-1} (7.65 eV) band in the solution is assigned to the second π-π^* transition (calculated at 7.35 eV). In the vapor phase, the second π-π^* band shifts to the shorter wavelengths. The theoretical result predicts that the weak band at ≈6.9 eV can be assigned to the first π-σ^* transition (calculated at 7.58 eV), and that the strong 8.27 eV band in the vapor phase is composed of the second π-π^* transition and the first σ-σ^* transition (calculated at 7.99 eV). Moreover, from the comparison between the observed and calculated results, the ≈8.8 eV band and the 9.7 eV band are assigned to the second (calculated at 8.97 eV) and third (calculated at 9.34 eV) σ-σ^* transitions, respectively.

Table 3 shows the theoretical results of the valence-shell transitions calculated for the symmetrical molecular structure of the enol form of HFAC, together with the observed values. The 4.64 eV band can be assigned to the first π-π^* transition (calculated at 4.48 eV). The weak band at ≈7.1 eV in the vapor phase is also observed in perfluorohexane, and is assigned to the first π-σ^* transition (calculated at 7.59 eV). The strong 7.90 eV band is ascribed to the superposition of the second π-π^* (calculated at 7.29 eV) and first σ-σ^* (calculated

TABLE 3. TRANSITION ENERGIES ($^1\Delta E$(eV)) AND OSCILLATOR STRENGTHS (f) OBSERVED AND CALCULATED FOR THE ENOL FORM OF HEXAFLUOROACETYLACETONE

Assignment	Obsd[a]		Calcd[b]		Main config.[c]
	$^1\Delta E$	f	$^1\Delta E$	f[d]	
$\sigma(n)$-π^*			2.65	0.000_8(z)	38—39
π-π^*	4.64	0.20	4.48	0.124(x)	37—39
$\sigma(n)$-π^*			4.85	0	38—40
σ-π^*			7.31	0	35—39
π-σ^*	≈7.1	≈0.02	7.59	0.011(z)	37—41
π-π^*	7.90	≈0.3	7.29	0.207(y)	37—40
$\sigma(n)$-σ^*			7.54	0.146(x)	38—41
σ-π^*			7.91	0.003(z)	34—39
σ-π^*			8.09	0	36—39 38—40
$\sigma(n)$-σ^*			8.17	0.004(y)	38—42
π-σ^*			8.44	0	37—42
π-σ^*			8.55	0.007(z)	37—43
$\sigma(n)$-σ^*	8.73	≈0.15	8.87	0.347(x)	38—43
σ-π^*			8.97	0.027(z)	28—39 35—40 34—39
π-σ^*			9.29	0.032(z)	37—44
$\sigma(n)$-σ^*			9.44	0.014(y)	38—45
$\sigma(n)$-σ^*	≈9.5		9.52	0.087(x)	38—44
π-π^*			9.83	0.235(y)	33—39

a) Observed value in the vapor phase. b) Calculated value for the symmetrical molecular structure of the enol form. c) Main electron configurations of the respective excited states are shown. d) The direction of the transition moment is shown in the parentheses, the x-axis being taken to be parallel to the O···H···O bond within the molecular (x-y) plane as is shown in Fig. 8(b).

TABLE 4. RESULTS OF THE CONFIGURATION ANALYSIS (WEIGHTS) FOR THE GROUND AND THE THIRD σ–σ^* EXCITED STATES OF THE ENOL FORM OF ACETYLACETONE[a]

	Structure	Reference Configuration[b,c]	State	
			Ground	Third σ–σ^*[d]
I	$(OH^-O^+)+(O^+H^-O)$[e]	i,j–36, 36	0.1101	—
II	$(OH^-O^+)-(O^+H^-O)$	i,j–36, 36	—	0.0999
III	(O–H···O)+(O···H–O)	i–36	0.4166	—
		i–36+π–π^*[f]	0.0194	0.1588
		i–36+σ–σ^*[f]	0.0153	0.1065
		(Total for sym. covalent structure)	(0.4513)	(0.2653)
IV	(O–H···O)−(O···H–O)	i–36	—	0.1892
		i–36+π–π^*[f]	—	0.0088
		i–36+σ–σ^*[f]	—	0.0061
		(Total for antisym. covalent structure)	—	(0.2041)
V	$O^{-1/2}H^+O^{-1/2}$	G^0[g]	0.3942	—
		π–π^*[h]	0.0184	0.1503
		σ–σ^*[h]	0.0153	0.1098
		i,j–k,l	0.0013	0.0190
		(Total for $O^{-1/2}H^+O^{-1/2}$ structure)	(0.4292)	(0.2791)
		Total	0.9906	0.8484
II+IV	Total for CT structure		—	0.3040

a) The results for the first π–π^* and the first σ–σ^* excited states are shown in Table 3 of Ref. 17. b) i and j denote the 20 occupied MO's of the anion, and k and l, the 15 vacant MO's of the anion. The 1s orbital of the hydrogen-bonded hydrogen is numbered as the 36th vacant orbital. c) i–k and i, j–k,l denote the singly and doubly excited reference configurations, respectively. d) The strong band observed at 8.08 eV in Fig. 2. e) The ionic structure, $((O^+H^-O)+(OH^-O^+))$, is also involved. f) Doubly excited configurations, i, j–k, 36. g) The ground reference configuration coincides with the ground state of the anion. h) Singly excited configurations, i–k.

at 7.54 eV) transitions. The shift to the longer wavelengths of the second π-π^* and first σ-σ^* bands of HFAC compared to the corresponding bands of TFAC is consistent with the theoretical predictions in Tables 2 and 3. The 8.73 eV band is safely assigned to the third σ-σ^* transition (calculated at 8.87 eV). The $\approx$9.5 eV band may tentatively be assigned to the fifth σ-σ^* transition (calculated at 9.52 eV).

Electronic Structures of the Intramolecular Hydrogen Bonds of Acetylacetone, TFAC, and HFAC. The previous paper[17] shows that the CT configuration characteristic of the intramolecular hydrogen bond corresponds to the one electron excitation from the nonbonding orbital to the antibonding orbital in the hydrogen bond. In the case of acetylacetone, the 20—26 configuration is the CT configuration (see Fig. 5 in Ref. 17.), and contributes mainly to the first π-π^* band (observed at 4.72 eV) (9.8%), the third σ-σ^* band (observed at 8.08 eV) (40.3%), and the fourth π-π^* band (observed at $\approx$9.8 eV) (16.3%). In acetylacetone, the third σ-σ^* band is richest in the CT character.

The CT character in the intramolecular hydrogen bond of acetylacetone was investigated quantitatively by the configuration analysis method; the result for the third σ-σ^* band is tabulated in Table 4, together with the result for the ground state (for the purpose of comparison, also see Table 3 in Ref. 17). In this table, the CT structure corresponds to the antisymmetric covalent structure IV and antisymmetric ionic structure II. Both structures contribute considerably (30.4%) to the third σ-σ^* excited state, revealing us that the band is rich in the CT character pertinent to the hydrogen bond.

Figures 4 and 5 show the energy levels of TFAC and HFAC, respectively, calculated by the modified CNDO-CI method for some low-lying π-π^* and σ-σ^* excited states of the enol form with the symmetrical molecular structures. In the figures, i–j represents a singly excited configuration caused by the one-electron excitation from

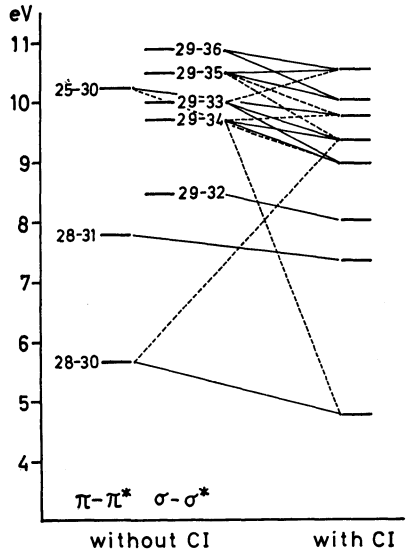

Fig. 4. Energy levels calculated with and without CI treatment for some lower π–π^* and σ–σ^* excited states of the enol form of TFAC.

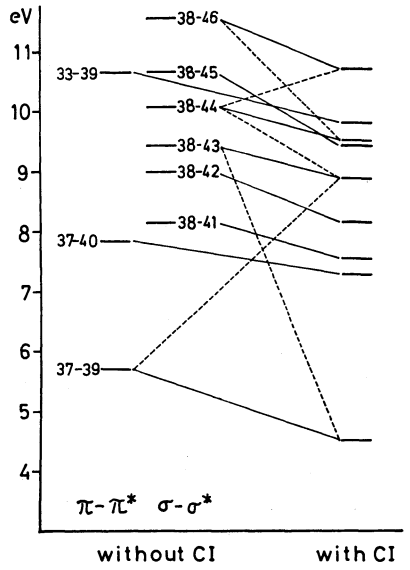

Fig. 5. Energy levels calculated with and without CI treatment for some lower π–π^* and σ–σ^* excited states of the enol form of HFAC.

the i-th occupied MO to the j-th vacant MO. From the shapes of the MO's of TFAC and HFAC (see Figs. 6 and 7), the CT configuration characteristic of the intramolecular hydrogen bond is the 29-34 configuration for TFAC and the 38-43 configuration for HFAC. As for TFAC, the 29-34 CT configuration interacts significantly with the 29-33 σ-σ^*, 25-30 π-π^*, and 28-30 π-π^* configurations, and contributes significantly to the first π-π^* (calculated at 4.75 eV), the second σ-σ^*

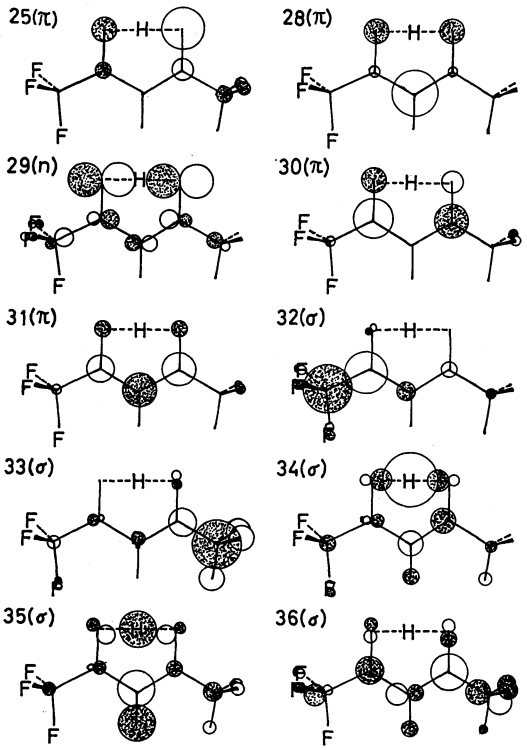

Fig. 6. Schematic shapes of some occupied and vacant MO's of the enol form of TFAC. The 29th MO is the highest occupied one.

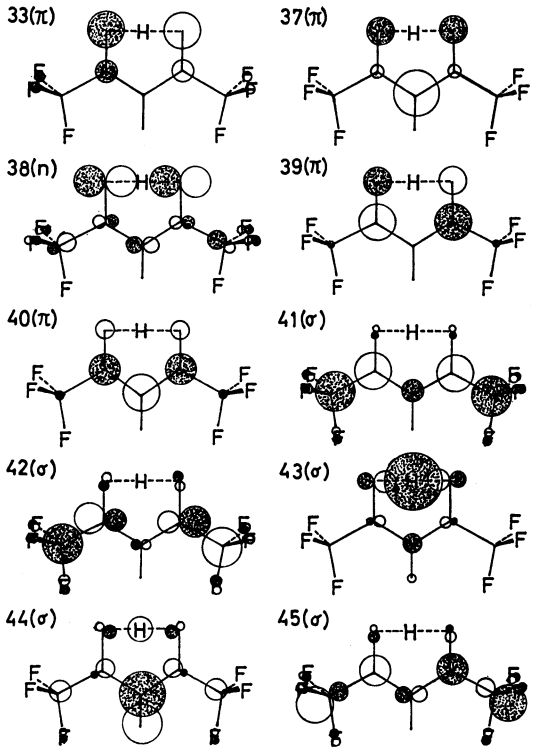

Fig. 7. Schematic shapes of some occupied and vacant MO's of the enol form of HFAC. The 38th MO is the highest occupied one.

(calculated at 8.97 eV), the third σ-σ* (calculated at 9.34 eV), and the third π-π* (calculated at 9.75 eV) excited states. The first π-π* band (observed at 4.55 eV) is mainly composed of the 28-30 π-π* (85.1%) and 29-34 CT (5.9%) configurations; the second σ-σ* band (observed at ≈8.8 eV), of the 29-34 CT (33.7%), 29-33 σ-σ* (31.8%), and 25-30 π-π* (11.4%) configurations; and the third σ-σ* band (observed at ≈9.7 eV), of the 29-33 σ-σ* (35.2%), 29-34 CT (22.0%), 29-35 σ-σ* (10.2%), and 28-30 π-π* (4.8%) configurations. The theoretical results calculated by the modified CNDO-CI method predict that the second and third σ-σ* bands are rich in the CT character pertinent to the hydrogen bond in TFAC.

In the case of HFAC, the 38-43 CT configuration interacts significantly with the 37-39 π-π* and 38-44 σ-σ* configurations, and contributes to the first π-π* (calculated at 4.48 eV) and the third σ-σ* (calculated at 8.87 eV) excited states. The first π-π* band (observed at 4.64 eV) is composed of the 37-39 π-π* (83.6%) and 38-43 CT (7.2%) configurations, and the third σ-σ* band (observed at 8.73 eV), of the 38-43 CT (67.4%), 38-44 σ-σ* (5.9%), and 37-39 π-π* (5.5%) configurations. The theoretical calculation predicts that the third σ-σ* band is the CT band characteristic of the intramolecular hydrogen bond of HFAC. It is noteworthy that the first π-π* bands of acetylacetone, TFAC, and HFAC observed at 4.5—4.7 eV have the CT character pertinent to the hydrogen bond by 5—10%.

Electron Densities of TFAC and HFAC. Figure 8 shows electron densities in the ground state calculated for the symmetrical molecular structures of the enol forms of TFAC and HFAC. By substituting the methyl

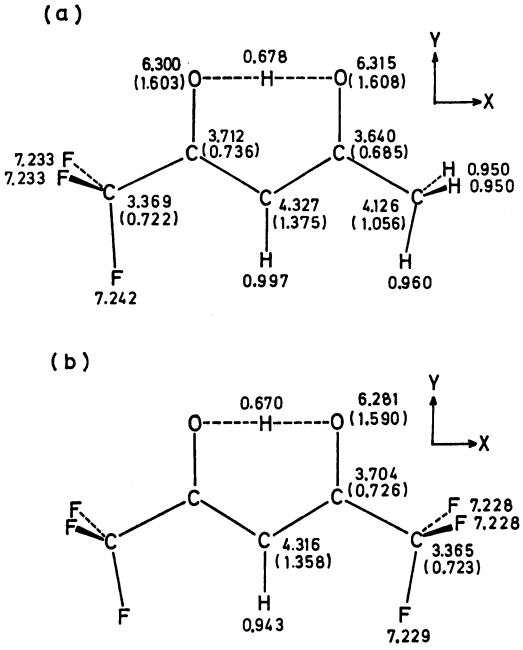

Fig. 8. Total and π-(in parentheses) electron densities calculated for the ground states of (a) TFAC and (b) HFAC.

group(s) by the trifluoromethyl group(s), the σ-electron density on the hydrogen-bonded hydrogen atom slightly decreases, and the π-electron densities increase on carbonyl carbon atoms with the decrease on oxygen atoms. The dipole moments of TFAC and HFAC were calculated to be 3.42 and 0.69 D, respectively. The cancellation between the dipole moments in the carbonyl groups and in the trifluoromethyl groups is responsible for the small dipole moment of HFAC.

The authors are indebted to Dr. J. Nakamura, the Institute of Physical and Chemical Research, for her helpful advice in modifying the VUV instrument. This work was partially supported by a Grant-in-Aid for Scientific Research from the Ministry of Education.

References

1) K. Nukasawa, J. Tanaka, and S. Nagakura, *J. Phys. Soc. Jpn.*, **8**, 792 (1953).
2) H. Tsubomura, *Bull. Chem. Soc. Jpn.*, **27**, 445 (1954).
3) C. A. Coulson, *Research*, **10**, 149 (1957).
4) F. B. van Duijneveldt and J. N. Murrell, *J. Chem. Phys.*, **46**, 1759 (1967).
5) S. Bratož, "Advances in Quantum Chemistry," Vol. 3, ed by P. O. Löwdin, Academic Press, New York (1967), p. 209.
6) P. A. Kollman and L. C. Allen, *Chem. Rev.*, **92**, 283 (1972).
7) K. Morokuma, S. Iwata, and W. A. Lathan, "The World of Quantum Chemistry," ed by R. Daudel and B. Pullman, D. Reidel, Dordrecht, Holland (1974); H. Umeyama and K. Morokuma, *J. Am. Chem. Soc.*, **99**, 1316 (1977), and references cited therein.
8) H. Tsubomura, *J. Chem. Phys.*, **23**, 2130 (1955); *ibid.*, **24**, 927 (1956).
9) S. Nagakura and M. Gouterman, *J. Chem. Phys.*, **26**, 811 (1957).

10) H. Ratajczak, *J. Phys. Chem.*, **76**, 3000, 3999 (1972); H. Ratajczak and W. J. Orville-Thomas, *J. Chem. Phys.*, **58**, 911 (1973); H. Ratajczak, W. J. Orville-Thomas, and C. N. R. Rao, *Chem. Phys.*, **17**, 197 (1976), and references cited therein.
11) R. S. Mulliken and W. B. Person, "Molecular Complexes," Wiley-Interscience, New York (1969).
12) S. Nagakura, *J. Chim. Phys.*, **61**, 217 (1964).
13) H. Morita, K. Fuke, and S. Nagakura, *Bull. Chem. Soc. Jpn.*, **50**, 645 (1977).
14) J. P. Schaefer and P. J. Wheatley, *J. Chem. Soc., A*, **1966**, 528.
15) A. L. Andreassen, D. Zebelman, and S. H. Bauer, *J. Am. Chem. Soc.*, **93**, 1148 (1971); A. L. Andreassen and S. H. Bauer, *J. Mol. Struct.*, **12**, 381 (1972).
16) A. H. Lowrey, C. George, P. D'Antonio, and J. Karle, *J. Am. Chem. Soc.*, **93**, 6399 (1971).
17) H. Nakanishi, H. Morita, and S. Nagakura, *Bull. Chem. Soc. Jpn.*, **50**, 2255 (1977).
18) R. N. Haszeldine, W. K. R. Musgrave, F. Smith, and L. M. Turton, *J. Chem. Soc.*, **1951**, 609.
19) E. M. Larsen, G. Terry, and J. Leddy, *J. Am. Chem. Soc.*, **75**, 5107 (1953).
20) R. L. Belford, A. E. Martell, and M. Calvin, *J. Inorg. Nucl. Chem.*, **2**, 11 (1956).
21) H. Morita, K. Fuke, and S. Nagakura, *Bull. Chem. Soc. Jpn.*, **49**, 922 (1976).
22) H. Baba, S. Suzuki, and T. Takemura, *J. Chem. Phys.*, **50**, 2078 (1968).
23) K. Kaya and S. Nagakura, *J. Mol. Spectrosc.*, **44**, 279 (1972).
24) J. E. Del Bene and W. L. Kochenour, *J. Am. Chem. Soc.*, **98**, 2041 (1976).
25) G. Karlström, B. Jönsson, B. Roos, and H. Wennerström, *J. Am. Chem. Soc.*, **98**, 6851 (1976).
26) D. E. Williams, *Acta Crystallogr.*, **21**, 340 (1966).
27) J. L. Burdett and M. T. Rogers, *J. Am. Chem. Soc.*, **86**, 2105 (1964).
28) R. L. Lintvedt and H. F. Holtzclaw, Jr., *J. Am. Chem. Soc.*, **88**, 2713 (1966).
29) M. B. Robin, "Higher Excited States of Polyatomic Molecules," Vol. 1, Academic Press, New York (1974).
30) C. Nishijima, H. Nakayama, T. Kobayashi, and K. Yokota, *Chem. Lett.*, **1975**, 5.